

Ferromagnetism and ferroelectricity in highly resistive $\text{Pb}_{0.7}\text{Sr}_{0.3}(\text{Fe}_{0.012}\text{Ti}_{0.988})\text{O}_3$ nanoparticles and its conduction by variable-range-hopping mechanism

Kuldeep Chand Verma,^{1,a)} M. Singh,¹ R. K. Kotnala,² and N. S. Negi¹

¹Department of Physics, Himachal Pradesh University, Shimla-171005, India

²National Physical Laboratory, New Delhi-110012, India

(Received 6 June 2008; accepted 30 July 2008; published online 20 August 2008)

The enhancement in ferromagnetism and ferroelectricity at room temperature for $\text{Pb}_{0.7}\text{Sr}_{0.3}(\text{Fe}_{0.012}\text{Ti}_{0.988})\text{O}_3$ (PSFT) nanoparticles is proved by magnetization and polarization hysteresis loop. The x-ray diffraction and micrograph show that the PSFT nanoparticles have distorted tetragonal single phase, and their average particle's size is 8 nm. The effect of Sr content reduces the particle size, and hence the multiferroic system becomes more resistive, which dominates the superparamagnetic/paraelectric relaxation. The variable-range-hopping conduction mechanism explained the high resistivity of PSFT nanoparticles, which suggests that the room temperature movement of electrons involves short-range order through defect states. © 2008 American Institute of Physics. [DOI: 10.1063/1.2973400]

The emerging trend of size reduction in nanomultiferroic system becomes more interesting in its field. In fact, the small nanomultiferroic systems have remarkable electric (i.e., spontaneous polarization) as well as magnetic (i.e., saturation magnetization) orders, which may be due to the short-range movement of electrons within the Fermi gap, and thus increase resistivity. These electromagnetite nanoparticles are used in data-storage media,¹ spintronic devices,² and multiple-stage memories.³ The most studied multiferroic systems of BiFeO_3 have low resistivity,⁴ which results in weak ferromagnetism⁵ and small polarization at room temperature.⁶ Li *et al.*⁷ reported the low resistivity in BiFeO_3 system, i.e., dependent on oxygen vacancies, low valence Fe ion due to their nonstoichiometric behavior and incomplete charge compensation, which may effect the distortion of the lattice. Rossiter *et al.*⁸ reported that the highly resistive magnetoelectric semiconductor attributes short-range interaction between the conduction and the localized spin electrons, which are highly disordered and contribute weak superparamagnetic/paraelectric relaxation. In our previous work of Fe-doped PbTiO_3 nanoparticles,⁹ the effect of polyvinyl alcohol (PVA) to reduce the particle size, which resulted in an increase in resistivity and improvement in ferromagnetism, was observed. The reported value of resistivity was in the order of 10^{10} Ω cm, which is higher than other multiferroic systems such as BiFeO_3 . The resistivity of Fe-doped PbTiO_3 system can further increase by reducing particle size with Sr substitution. Pontes *et al.*¹⁰ reported the effect of Sr doping in PbTiO_3 to reduce grain size because the Sr content attributes lower grain-growth rates due to the slower diffusion of Sr^{2+} with Pb^{2+} ion. The substitutions of Sr at Pb site and Fe at Ti site may provide relaxation stability and interesting transport properties. In literature,^{11,12} different stabilized relaxation processes were studied with varying temperature by a variable-range-hopping (VRH) conduction mechanism, which was employed when the conduction band

is absent, and the extended states are far away from the Fermi level.

In this letter, we report the enhanced ferromagnetic and ferroelectric properties of highly resistive $\text{Pb}_{0.7}\text{Sr}_{0.3}(\text{Fe}_{0.012}\text{Ti}_{0.988})\text{O}_3$ (PSFT) nanoparticles by VRH conduction mechanism. The PSFT nanoparticles has been prepared by using chemical route and PVA as surfactant. The details of material processing were given elsewhere.⁹ The structural and microstructural characterizations have been carried out by x-ray diffraction (XRD) (using X-Pert PRO) and transmission electron microscopy (TEM) (using Hitachi H-7500). The electrical measurements were carried out on PSFT pellet sample sintered at 1000 °C in the temperature range of 298–470 K by using Keithley 2611 source meter. For these measurements, Ag contact was deposited on both the surface of pellet as top and bottom electrodes. The saturation magnetization was measured on the powder sample of PSFT sintered at 700 °C by using VSM-735. The electrical polarization was carried out on poled pellet samples sintered at 700 and 1000 °C by using Radiant Technologies ferroelectric test system.

The XRD pattern indicates the distorted tetragonal ($c/a \sim 1.0032$) single phase of PSFT nanoparticles heated at 700 °C for 2 h [Fig. 1(a)]. The observed relative intensity of (101) peak is large, when comparing it to standard $\text{Pb}(\text{Fe},\text{Ti})\text{O}_3$. This implies that the crystal growth occurs along the (101) direction, and the distorted structure is very close to cubic, indicating the uniformity in the close packing of grains. The average particle's size calculated from XRD peak using Scherrer's formula¹³ is 8 nm. The observed particle size is smaller than that reported as 30 nm in our previous system of $\text{Pb}(\text{Fe}_{0.012}\text{Ti}_{0.988})\text{O}_3$.⁹ The reduction in particle size is due to Sr content, which is discussed earlier in the previous section. When the nanoparticles are sufficiently uniform in size, they self-assemble in close-packed, ordered nanoparticles superlattices, which can reduce the effect of superparamagnetic/paraelectric.¹⁴ This is well illustrated in Fig. 1(b), which shows a TEM image of PSFT nanoparticles, i.e., average particle's size is 7 nm.

^{a)}Electronic mail: kuldeep0309@yahoo.co.in.

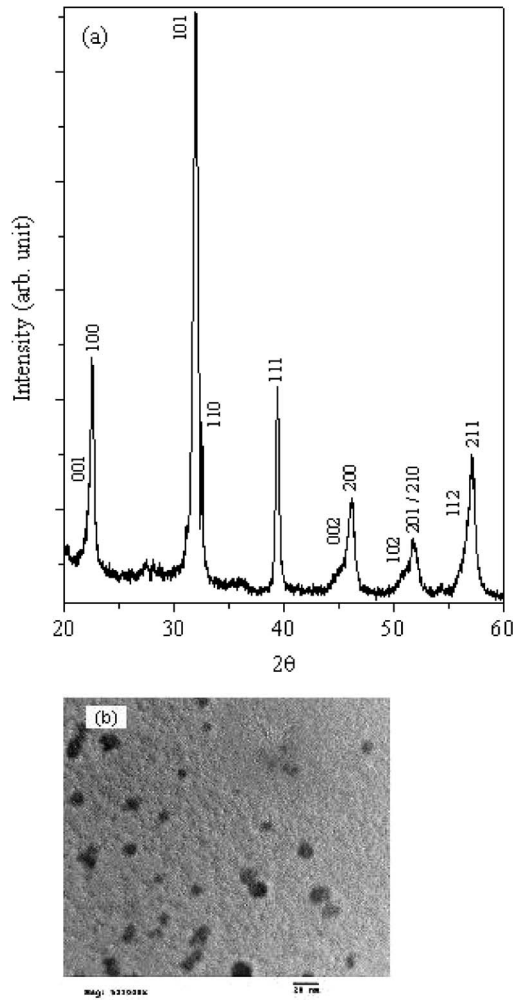


FIG. 1. (a) XRD pattern and (b) TEM of PSFT nanoparticles heated at 700 °C for 2 h.

The ferromagnetic properties of PSFT nanoparticles at room temperature shows a saturation magnetization, (M_s) $\sim 64.4 \times 10^{-3}$ emu/g ($0.81 \mu_B/\text{Fe}$), and coercive field (H_c) ~ 35 Oe [Fig. 2(a)]. This value of coercive field is very small as compared to some $\text{Pb}(\text{Fe}, \text{Ti})\text{O}_3$ system of nanoparticles.^{9,15} The similar behavior was also found in $\text{Pb}(\text{Fe}, \text{W})\text{TiO}_3$ system of thin film.¹⁶ It is reported that the spin canting due to small distortion between $\text{Fe}^{3+}-\text{O}-\text{Fe}^{3+}$ spins, results in weak ferromagnetism. Sr^{2+} ion in PSFT reduces the particles size as well as the degree of distortion. The alignment of grains might be uniform, which can raise resistivity within field ions, and hence the superparamagnetic behavior will be reduced. This type of ferromagnetic behavior was explained by Coey *et al.*² for their system of Fe-doped SnO_2 , This suggested that the electrons trapped into oxygen vacancies via F -center. In addition, the charge compensation required by doping of Sr^{2+} ion might result in the formation of Fe^{4+} or oxygen vacancies; the former may distribute statistically with Fe^{3+} ion and lead to improve ferromagnetism.¹⁷

Figures 2(b) and 2(c) show the ferroelectric properties of the PSFT nanoparticles at room temperature sintered at 700 and 1000 °C, respectively. At 50 Hz the frequency of polarization and maximum applied electric field of ± 15 kV/cm, spontaneous polarization $P_s \sim 8.5 \mu\text{C}/\text{cm}^2$, remanent polarization $P_r \sim 8.1 \mu\text{C}/\text{cm}^2$, and coercive field

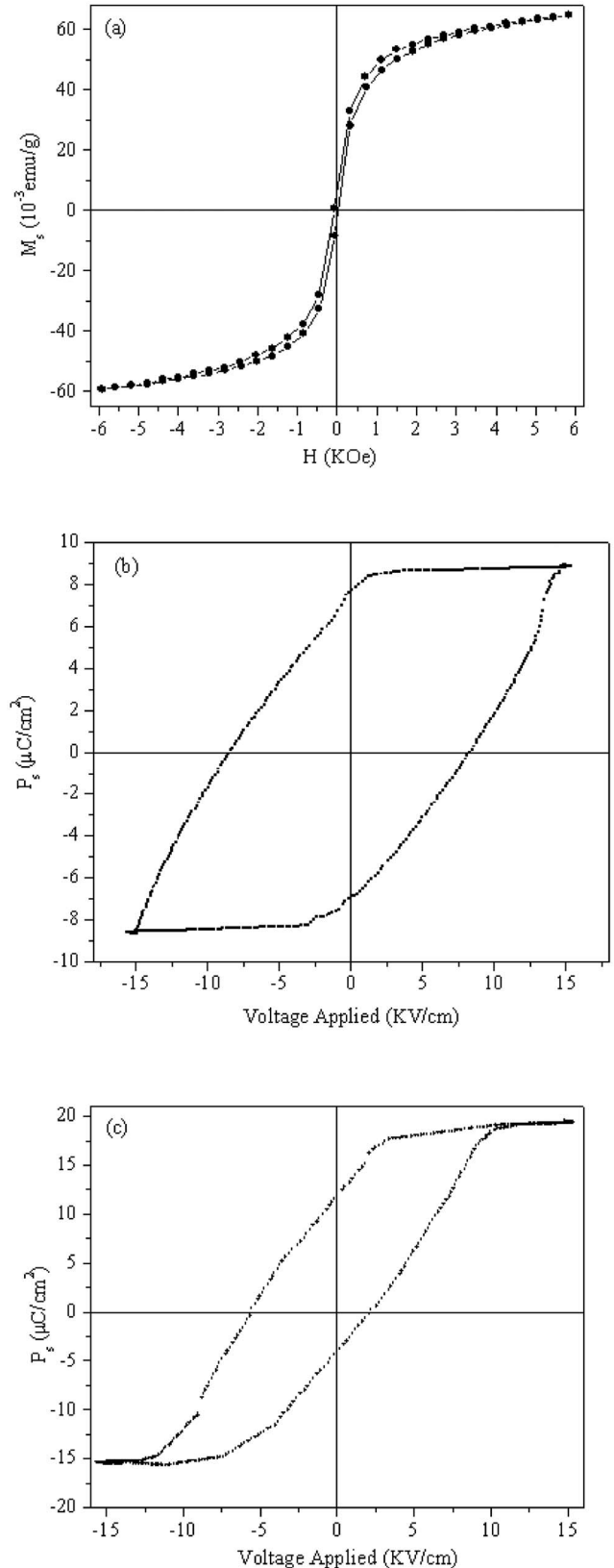


FIG. 2. (a) Saturation magnetization (M_s) vs magnetizing field (h) (powder sample sintered at 700 °C) (b) Spontaneous polarization (P_s) vs applied voltage (pellet sample sintered at 700 °C) and (c) P_s vs applied voltage (pellet sample sintered at 1000 °C) for PSFT nanoparticles at room temperature.

$E_c \sim 10$ KV/cm for PSFT pellet sintered at 700 °C. When the PSFT pellet sintered at 1000 °C, the values of spontaneous polarization $P_s \sim 20.7 \mu\text{C}/\text{cm}^2$, remanent polarization $P_r \sim 13.3 \mu\text{C}/\text{cm}^2$, and coercive field $E_c \sim 5.7$ kV/cm are

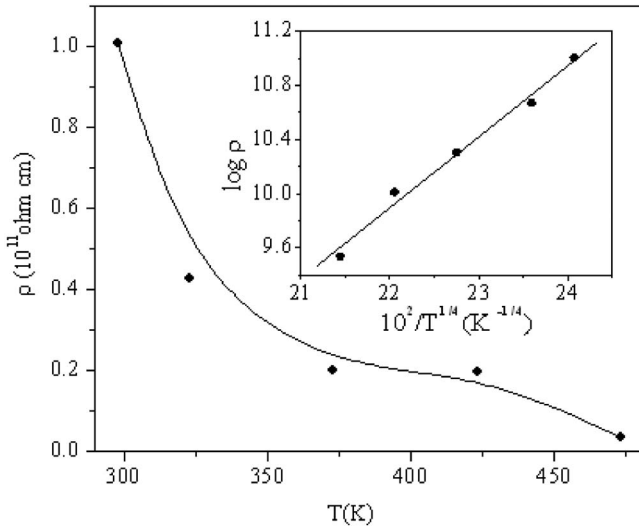


FIG. 3. Variation in dc resistivity (ρ) with temperature. Plot of $\log \rho$ vs $10^2/T^{1/4}$ ($k^{-1/4}$) (inset).

observed. The small values of polarization observed at a low sintered temperature of 700 °C indicate the existence of porosity in the PSFT pellet. This porosity may be created by PVA, when used as binder during pellet formation process. Compared with the results reported by Palkar *et al.*¹⁸ for $\text{Pb}(\text{FeTi})\text{O}_3$ system, the present system of Sr-doped $\text{Pb}(\text{Fe}, \text{Ti})\text{O}_3$ shows better spontaneous polarization. This improvement may be attributed to small particles, which can easily control crystalline structure, defects, oxygen vacancies, and stoichiometry.

Figure 3 shows temperature dependent dc resistivity of PSFT nanoparticles. The observed value of resistivity lies in the order of $10^{11} \Omega \text{ cm}$, which is quite higher than other multiferroic systems such as BiFeO_3 . The general exponential fitting of resistivity with temperature ($1/T$) cannot explain the conduction band, because the calculated value of activation energy is less than the parent PbTiO_3 and SrTiO_3 . The activation energy up to 470 K is much less than half of the band gap, indicating extrinsic conduction, i.e., the conduction band is absent and the electrons transport takes place within Fermi gap through defect states.

Mott and Davis¹⁹ explained these defect states by a VRH conduction mechanism that holds in the present system by fitting resistivity under different exponents of temperature. The best fitting and satisfactory result is obtained by using

$$\rho = \rho_0 \exp(BT^{-1/4}), \quad (1)$$

where $B=4E/(K_B T^{3/4})$ and E is the activation energy for VRH. The plot $\log_{10}(\rho_{\text{dc}})$ versus $T^{-1/4}$ over a considerable temperature range shows a straight line [Fig. 3 (inset)]. To analyze VRH conduction, the PSFT semiconductor behaves like amorphous materials at room temperature due to states in the gap because of divacancies and dangling bonds. It depends on factors such as Pb vacancies, Sr vacancies due to slower diffusion of Sr^{2+} ion; oxygen vacancies, and Ti that can easily change its valence. This result in electron jump between $\text{Ti}^{4+} \leftrightarrow \text{Ti}^{3+}$ and/or $\text{Fe}^{4+} \leftrightarrow \text{Fe}^{3+}$ might be possible.

As a result, the path of electrons formed by optimal pair hopping rate from one localized state to another through short range in the disorder system. Above room temperature, the concentrations of magnetic ions and their clusters links increase and result in a long-range movement of electrons. The activation energy by VRH mechanism is $E=0.98 \text{ meV}$ in the lower temperature region of 300 K, which increases to 1.05 meV at 470 K. A similar behavior was also obtained by Ang *et al.*²⁰ This suggested that the hopping of electrons at or below room temperature involves short-range movement. At higher temperature it involves long-range movement, which gives dc conduction.

In summary, we have studied the effect of Sr content to reduce the particles size in chemically prepared PSFT nanoparticles. The XRD and micrograph show that the average particle's size is 8 nm. The improvement in saturation magnetization $M_s \sim 64.4 \times 10^{-3} \text{ emu/g}$ and spontaneous polarization $P_s \sim 20.7 \mu\text{C/cm}^2$ are observed at room temperature. The high resistivity (in the order of $10^{11} \Omega \text{ cm}$) of PSFT particles suggests that the band conduction is absent, and their transport mechanism can be explained by VRH. The observed VRH mechanism shows that the short-range movement of electrons takes place at room temperature, whereas at higher temperature region, it involves long-range order.

- ¹J. Hemberger, P. Lunkenheimer, R. Fichtl, H. A. Nidda, V. Tsurkan, and A. Loidl, *Nature (London)* **434**, 364 (2005).
- ²J. M. D. Coey, A. P. Douvalis, C. B. Fitzgerald, and M. Venkatesan, *Appl. Phys. Lett.* **84**, 1332 (2004).
- ³T. Kimura, Y. Sekio, H. Nakamura, T. Siegrist, and A. P. Ramirez, *Nat. Mater.* **7**, 291 (2008).
- ⁴R. Schmidt, W. Eerenstein, T. Winiacki, F. D. Morrison, and P. A. Midgley, *Phys. Rev. B* **75**, 245111 (2007).
- ⁵Y. P. Wang, L. Zhou, M. F. Zhang, Y. Y. Chen, J. M. Liu, and Z. G. Liu, *Appl. Phys. Lett.* **84**, 1731 (2004).
- ⁶S. Y. Tan, S. R. Shannigrahi, S. H. Tan, and F. E. H. Tay, *J. Appl. Phys.* **103**, 09405 (2008).
- ⁷M. Li, M. Ning, Y. Ma, Q. Wu, and C. K. Ong, *J. Phys. D* **40**, 1603 (2007).
- ⁸P. L. Rossiter, *The Electrical Resistivity of Metals and Alloys* (Cambridge University Press, Cambridge, 1987).
- ⁹K. C. Verma, R. K. Kotnala, and N. S. Negi, *Appl. Phys. Lett.* **92**, 152902 (2008).
- ¹⁰F. M. Pontes, S. H. Leal, M. R. Santos, E. R. Leite, E. Longo, L. E. Soledade, A. J. Chiquito, M. A. Machado, and J. A. Varela, *Appl. Phys. A* **80**, 875 (2005).
- ¹¹M. A. Chernikov, L. Degiorgi, E. Felder, S. Paschen, A. D. Bianchi, H. R. Ott, J. L. Sarrao, Z. Fisk, and D. Mandrus, *Phys. Rev. B* **56**, 1366 (1997).
- ¹²L. Steinke, D. Schuh, M. Bichler, G. Abstreiter, and M. Grayson, *Phys. Rev. B* **77**, 235319 (2008).
- ¹³B. D. Cullity, *X-Ray Diffraction* (Addison-Wesley, Reading, MA, 1967).
- ¹⁴M. K. Roy, B. Haldar, and H. C. Verma, *Nanotechnology* **17**, 232 (2006).
- ¹⁵Z. Ren, G. Xu, X. Wei, Y. Liu, X. Hou, P. Du, W. Weng, G. Shen, and G. Han, *Appl. Phys. Lett.* **91**, 063106 (2007).
- ¹⁶A. Kumar, I. Rivera, R. S. Katiyar, and J. F. Scott, *Appl. Phys. Lett.* **92**, 132913 (2008).
- ¹⁷T. Matsui, H. Tanaka, N. Fujimura, N. Ito, H. Mabuchi, and K. Morii, *Appl. Phys. Lett.* **81**, 2764 (2002).
- ¹⁸V. R. Palkar and S. K. Malik, *Solid State Commun.* **134**, 783 (2005).
- ¹⁹N. F. Mott and E. A. Davis, *Electronic Processes in Non-Crystalline Materials* (Clarendon, Oxford, 1979).
- ²⁰C. Ang, Z. Yu, Z. Jing, P. Lunkenheimer, and A. Loidl, *Phys. Rev. B* **61**, 3922 (2000).